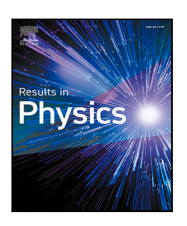
ELSEVIER

Contents lists available at ScienceDirect

### **Results in Physics**

journal homepage: www.elsevier.com/locate/rinp





## Dynamic of Si nanoparticles inside of a quadrupolar trap: Analysis of the angular momentum transfer

Luis Carretero a,\*, Pablo Acebal a, Salvador Blaya a, Manuel Pérez-Molina b

- a Departamento de Ciencia de Materiales. Óptica y Tecnología Electrónica Universidad Miguel Hernández. 03202 Elche. Spain
- <sup>b</sup> Departamento de Física, Ingeniería de Sistemas y Teoría de la Señal, Escuela Politécnica Superior, Instituto Universitario de Física Aplicada a las Ciencias y las Tecnologías, Universidad de Alicante., Spain

#### ARTICLE INFO

# Keywords: Optical forces Mie resonances Silicon nanoparticles Ouadrupolar forces

#### ABSTRACT

We investigate the dynamics of Si spherical nanoparticles for different infrared wavelengths in a system based on two circularly polarized counter-propagating Gaussian beams. Through the analysis of the dipolar and quadrupolar forces, we obtain several conditions under which these nanoparticles describe different types of attractive or repulsive spirals at focus plane depending on the efficiency of the quadrupole trap obtained. We demonstrate that these spirals are generated by the angular momentum transfer from the electromagnetic field to the particles, and this is mainly due to the interference forces dipole–dipole and quadrupole–dipole. Through the adequate selection of the wavelength, angular momentum transfer can only take place with quadrupolar-dipolar interference forces. We study particle dynamics by solving the deterministic and non-deterministic over-damped Langevin equation.

#### 1. Introduction

The study of silicon nanoparticles is an important topic in the field of photonics and optics because such particles present high resonances with low dissipation levels, are biologically compatible and can be produced at low cost [1]. Moreover, silicon nanoparticles have been used in different fields [1] such as wavefront control, optical switching, harmonic generation or for increasing solar cells efficiency [2]. The changes in spin and orbital momentum when an electromagnetic field is scattered by a Si particle result in a radiation force on it [3]. In the case of nanoparticles, these optical forces have been studied in depth [4-6]; spin and orbital momentum have a very important role in this, which has also been widely studied. Specifically, in the review of Ref. [7], optical angular momentum is analyzed from the perspective of canonical angular momentum, which makes it possible to describe the main theoretical and experimental results in this field. Thus, the transference of spin or orbital angular momentum from the electromagnetic field to the particles is one of the main research interest in this field. For example, it has been demonstrated that spin angular momentum can accelerate and decelerate the orbital motion of nanoparticles by using circularly polarized Laguerre-Gaussian beams [8]. Vortex beams with circular or radial polarization have also been used for spinning and orbiting micro-sized particles [9], whereas Laguerre-Gaussian beams have been employed to analyze the scattering conversion between spin and orbital angular momentum to

induced torques on microparticles [10]. Orbital angular momentum can be efficiently transferred between electron Gaussian beams and chiral plasmon-supporting thin films [11]. Moreover, the mechanical action of the spin part of internal energy flow and its ability to cause translational (orbital) motion was experimentally demonstrated in [12-14] and prior to this it was theoretically described in [6,15]. Using strongly focused LG10 optical beams, Zhao et al. [16] have demonstrated spin to orbital momentum conversion on gold particles by analyzing the resulting rotation of the trapped nanoparticles. Furthermore, previous angular momentum transfer studies were analyzed in a framework where the interaction of dipole with electromagnetic field explained the theoretical and experimental results. Another very important and deeper review that covers the majority of optical force mechanisms from a theoretical and experimental point of view can be found in [17]. On the other hand, particle dynamics due to optical force inside optical traps have been studied by different authors. For example, a study has been carried out of the transversal trajectories of Si micro-particles in Bessel beam traps [18], Lissajous-like trajectories have also been described in [19]. Furthermore, particle dynamics as a function of the topological charge of Laguerre-Gaussian beams are studied in [20] in order to demonstrate the transfer of angular momentum to microparticles in vacuum. The different dynamics of particles in optical vortices have been theoretically analyzed in [21], whereas, the stability of trajectories inside a Bessel beam depending on ambient damping

E-mail address: l.carretero@umh.es (L. Carretero).

<sup>\*</sup> Corresponding author.

has been studied in Ref. [22]. Particle dynamics have also been studied in a courter-propagating system since the earliest studies in this field [23], and recently, this configuration [24] has been used to study the dynamics of silicon nanowires. In Ref. [25], a 4Pi focusing system has been used to obtain (among other results) spiral trajectories by switching an adequate phase modulation of the incident beams. Recently, the importance of multipole excitations [26] has been pointed out in different papers, where the following have been analyzed: the optical pulling force produced by the interference of the radiation multipoles [27], resonant electromagnetic dipole-quadrupole coupling in nanoparticle arrays [28] or the angular momentum transfer between a quadrupole emitter and a dipole acceptor [29]. Finally Refs. [30] and [1] have proposed different optical sorting techniques which include the quadrupolar forces. In this paper, we study the dynamics of Si nanoparticles inside an infrared quadrupolar optical trap by solving the Langevin equation. We also analyze the angular momentum transfer from the electromagnetic field to mechanical angular momentum of Si nanoparticles mainly via the interference forces of dipole-dipole and quadrupole-dipole radiation.

#### 2. Theory

Let us assume two circularly polarized counter-propagating Gaussian beams given by [31]:

$$\mathbf{E} = \omega \left( i \psi_{-} \hat{\mathbf{x}} - \psi_{-} \hat{\mathbf{y}} + \frac{1}{k} \nabla_{T} \psi_{+} \hat{\mathbf{z}} \right)$$
 (1)

$$\mathbf{H} = \frac{k}{\mu_0} \left( \psi_+ \hat{\mathbf{x}} + i \psi_+ \hat{\mathbf{y}} - \frac{i}{k} \nabla_T \psi_- \hat{\mathbf{z}} \right) \tag{2}$$

where

$$\psi_{\pm} = (u_{-} \exp(ikz) \pm u_{+} \exp(-ikz)) \tag{3}$$

and  $u_{+}$  is the fundamental gaussian mode given by:

$$u_{\pm} = \frac{A_0 z_R}{\pm z + i z_P} exp\left(\frac{-ik(x^2 + y^2)}{2(\pm z + i z_P)}\right) \tag{4}$$

 $A_0$  is the amplitude of potential vector [31] and  $z_R$  is the confocal parameter whose relation with the beam waist  $w_0$  is  $z_R = kw_0^2/2$ , k being the wave number in water (with refractive index n) and  $\nabla_T =$  $\partial_x + i\partial_y$ .

Under these conditions, we are going to analytically demonstrate that Si particles at the focus plane describe different types of spirals, circles or straight lines, which implies that they have acquired orbital angular momentum from the electromagnetic field except when the trajectory is a straight line. Particle dynamics and the angular moment acquired by them are strongly determined by the balance of dipolar and quadrupolar forces, so this dynamic can be used to determine which type of forces are dominant. In order to demonstrate this, we have used the time-average optical forces obtained in Ref. [27] including high order forces [27,30] related to multipolar expansion; i.e. by taking into account electric and magnetic quadrupoles. The total force  $\mathbf{F}_T$  can be expressed as the sum of dipolar forces  $\mathbf{F}_d$  and quadrupole forces  $\mathbf{F}_a$ :

$$\mathbf{F}_T = \mathbf{F}_d + \mathbf{F}_a \tag{5}$$

where

$$\mathbf{F}_d = \mathbf{F}_p + \mathbf{F}_m + \mathbf{F}_{pm} \tag{6}$$

$$\mathbf{F}_q = \mathbf{F}_Q + \mathbf{F}_M + \mathbf{F}_{Qp} + \mathbf{F}_{Mm} \tag{7}$$

$$\mathbf{F}_{p} = \frac{1}{2} \Re[(\nabla \mathbf{E}^{*}).\mathbf{p}]; \, \mathbf{F}_{m} = \frac{1}{2} \Re[(\nabla \mathbf{B}^{*})\mathbf{m}]$$
(8)

$$\mathbf{F}_{Q} = \frac{1}{4} \Re[(\nabla \nabla \mathbf{E}^{*}) : \mathbf{Q}]; \, \mathbf{F}_{M} = \frac{1}{4} \Re[(\nabla \nabla \mathbf{B}^{*}) : \mathbf{M}]$$
(9)

$$\mathbf{F}_{pm} = -\frac{k^4}{12\pi\epsilon_0 c} \Re[\mathbf{p} \times \mathbf{m}^*]; \, \mathbf{F}_{Qp} = -\frac{k^5}{40\pi\epsilon_0} \Im[\mathbf{Q} \cdot \mathbf{p}^*]$$
 (10)

$$\mathbf{F}_{Mm} = -\frac{k^5}{40\pi\varepsilon_0 c^2} \mathfrak{F}[\mathbf{M}.\mathbf{m}^*] \tag{11}$$

where E and B =  $\mu_0$ H are given by Eqs. (1)-(2), p,Q, m and M are the electric dipole, electric quadrupole, magnetic dipole and the magnetic quadrupole respectively, given by:  $\mathbf{p} = \alpha_e \mathbf{E}, \mathbf{m} = \alpha_m \mathbf{B}, \mathbf{Q} =$  $\frac{\alpha_Q}{2}(\nabla \mathbf{E} + (\nabla \mathbf{E})^T), \mathbf{M} = \frac{\alpha_M}{2}(\nabla \mathbf{B} + (\nabla \mathbf{B})^T) [27], \ \alpha_e = 6i\pi\epsilon_0 a_1 n^2 / k^3, \ \alpha_m =$  $6i\pi b_1/(k^3\mu_0)$ ,  $\alpha_O = 40i\pi \epsilon_0 a_2 n^2/k^5$  and  $\alpha_M = 40i\pi b_2/(k^5\mu_0)$ ,  $a_1, b_1, a_2$  and  $b_2$  being the Mie coefficients [4]. Finally n is the water refractive index, and  $\Re[]$ ,  $\Im[]$  denote real and imaginary part respectively.

By introducing Eqs. (1)-(2) into (8)-(11), and evaluating them at the focus plane (z = 0) we obtain in cylindrical coordinates that:

$$\mathbf{F}_{d} = F(r) \left( (A_d + B_d r^2) \hat{r} + C_d \hat{\theta} \right) = F_d^r(r) \hat{r} + F_d^{\theta}(r) \hat{\theta}$$
 (12)

$$\mathbf{F}_{q} = F(r)\left((A_{q} + B_{q} r^{2})\hat{r} + C_{q}\hat{\theta}\right) = F_{q}^{r}(r)\hat{r} + F_{q}^{\theta}(r)\hat{\theta}$$

$$\tag{13}$$

where we have defined the radial function:

$$F(r) = A_0^2 exp\left(\frac{-kr^2}{z_R}\right) k^2 r \tag{14}$$

and the coefficients are given by:

$$A_d = A_p + A_m + A_{pm} \tag{15}$$

$$A_{q} = A_{O} + A_{M} + A_{Op} + A_{Mm} (16)$$

$$B_d = B_p + B_m + B_{pm} (17)$$

$$B_q = B_Q + B_M + B_{Qp} + B_{Mm} (18)$$

$$C_d = C_p + C_m + C_{pm} \tag{19}$$

$$C_q = C_Q + C_M + C_{Qp} + C_{Mm} (20)$$

where suffixes refer to the contribution to dipolar and quadrupolar coefficients (A, B, C) of electric dipolar force (p), magnetic dipolar force (m), interference electric-magnetic dipolar force (pm), quadrupolar electric force (Q), quadrupolar magnetic force (M), interference of dipole-dipole and quadrupole-dipole forces quadrupolar-dipolar electric force (Qp) and interference quadrupolar-dipolar magnetic force (Mm). Their values are:

$$A_{p} = \frac{2c^{2}\Re\left[\alpha_{e}\right]}{z_{p}^{2}n^{2}} \qquad A_{m} = \frac{-4k\Re\left[\alpha_{m}\right]}{z_{R}} \qquad A_{pm} = -\frac{4k^{4}\Re\left[\alpha_{e}\alpha_{m}^{*}\right]\mu_{0}c^{2}}{3\pi z_{R}n}$$
(21)

$$B_{p} = -\frac{2kc^{2}\Re[\alpha_{e}]}{z_{R}^{3}n^{2}} \qquad B_{m} = 0$$
 (22)

$$C_{p} = \frac{2c^{2}\Im[\alpha_{e}]}{z_{o}^{2}n^{2}} \qquad C_{m} = 0 \qquad C_{pm} = \frac{k^{4}\mu_{0}c^{2}\Re[\alpha_{e}\alpha_{m}^{*}]}{3z_{R}\pi n} \quad (23)$$

$$A_Q = -\frac{\Re[\alpha_Q]c^2k(s-4)(s-2)}{z_R^3n^2} \qquad A_M = -\frac{\Re[\alpha_M](s(8-5s)-8)}{2z_R^4}$$
 (24)

$$A_{Q} = -\frac{\Re[\alpha_{Q}]c^{2}k(s-4)(s-2)}{z_{R}^{3}n^{2}} \qquad A_{M} = -\frac{\Re[\alpha_{M}](s(8-5s)-8)}{2z_{R}^{4}}$$
(24)
$$A_{Qp} = -\frac{c^{2}k^{5}(s-2)\Im[\alpha_{Q}\alpha_{e}^{*}]}{20\pi z_{R}^{2}n^{2}\epsilon_{0}} \qquad A_{Mm} = \frac{k^{6}3n^{2}\Im[\alpha_{M}\alpha_{m}^{*}]}{20\pi z_{R}c^{2}n^{2}\epsilon_{0}}$$
(25)
$$B_{Q} = -\frac{\Re[\alpha_{Q}]c^{2}k^{2}(4s-13)}{2z_{R}^{4}n^{2}} \qquad B_{M} = -\frac{\Re[\alpha_{M}]k(s(5s-12)+16)}{2z_{R}^{5}}$$
(26)

$$B_Q = -\frac{\Re[\alpha_Q]c^2k^2(4s-13)}{2z_R^4n^2} \qquad \qquad B_M = -\frac{\Re[\alpha_M]k(s(5s-12)+16)}{2z_R^5}$$
 (26)

$$B_{Qp} = \frac{3c^2 k^6 \Im[\alpha_Q \, \alpha_e^*]}{40\pi z^3 \, n^2 \epsilon_5} \qquad B_{Mm} = 0 \tag{27}$$

$$C_Q = 0$$
  $C_M = \frac{\Im{\{\alpha_M\} (s^2 - 8s + 8\}}}{2z_p^4}$  (28)

$$C_{Q} = 0 C_{M} = \frac{\Im[\alpha_{M}] \left(s^{2} - 8s + 8\right)}{2z_{R}^{4}} (28)$$

$$C_{Qp} = \frac{c^{2}k^{5}(s - 2)\Re[\alpha_{Q} \alpha_{e}^{*}]}{20\pi z_{R}^{2}n^{2}\epsilon_{0}} C_{Mm} = \frac{k^{6}\Re[\alpha_{M} \alpha_{m}^{*}]}{20\pi z_{R}c^{2}\epsilon_{0}} (29)$$

 $s = z_R k$  being an adimensional parameter. To obtain Eqs. (12)–(13) from the exact ones, we have neglected the terms dependent on  $r^2$ in the azimuthal forces and higher than  $r^3$  in the radial quadrupolar forces  $\mathbf{F}_O$  and  $\mathbf{F}_M$ . It is important to note that Eqs. (12) and (13) have neither axial component nor dependence on the azimuthal coordinate  $\theta$ , so the particles will be trapped at focus plane (z = 0) for any radial and azimuthal position.

Azimuthal forces  $F_d^\theta = C_d F(r)$  and  $F_q^\theta = C_q F(r)$  transfer angular momentum from the electromagnetic field to the particles, so, taking into account that  $C_m = C_Q = 0$ , we can affirm that dipolar

L. Carretero et al. Results in Physics 19 (2020) 103520

magnetic forces and quadrupolar electric forces do not contribute to the angular momentum transfer when counter-propagating circularly polarized gaussian beams are used. Magnetic dipolar forces do not transfer angular momentum because the magnetic orbital angular momentum associated to the magnetic field given by Eq. (2) is null [6]. Furthermore, the radial dependence in both cases is the same (F(r)), but the coefficients  $C_d$  and  $C_q$  depend on dipolar and quadrupolar polarizabilities respectively, then, the total azimuthal force  $F_T^{\theta} = F_d^{\theta} +$  $F_q^{\theta} = F(r)(C_d + C_q)$ , could be positive, negative or null according to the values of  $(C_d + C_q)$ . Therefore, the angular momentum transfer from the electromagnetic field to the particles could be controlled by balancing the dipolar and quadrupolar forces. To do this, for a fixed particle radius, balance between dipolar and quadrupolar forces could be obtained by varying the wavelength of the incident electromagnetic

In the same way as azimuthal forces, radial forces  $F_d^r$  and  $F_a^r$ also show the same radial dependence that can be controlled by the radiation wavelength for obtaining attractive, repulsive or null forces.

In the next section we are going to analyze the influence of quadrupolar interaction on particle dynamics.

#### 2.1. Particle dynamics

As it is widely used, we will assume that the viscous forces in water dominate the inertia forces thus, the dynamics of Si nanoparticles can be described by the overdamped Langevin equation [32,33] given by:

$$\gamma \frac{d\mathbf{R}}{dt} = \mathbf{F}_T(\mathbf{R}) + \mathbf{W}(t) \tag{30}$$

where **R** is the position vector of a particle,  $\gamma \frac{d\mathbf{R}}{dt}$  is the frictional force of a particle, ( $\gamma = 6\pi v r_a$ ,  $r_a$  is the particle radius and  $v = 8.9 \ 10^{-4} Pa \ s$  is the water viscosity),  $\mathbf{F}_T(\mathbf{R})$  is the optical force given by Eqs. (5)–(13) and  $\mathbf{W}(t)$  is a time dependent random force that causes Brownian motion.

By introducing Eqs. (12)-(13) into (30), we can obtain the deterministic overdamped Langevin equation (W(t) = 0):

$$\frac{dr}{dt} = F_T^r(r) = (Ar + Br^3)f(r)$$

$$\frac{d\theta}{dt} = F_T^{\theta}(r) = Cf(r)$$
(31)

$$\frac{d\theta}{dt} = F_T^{\theta}(r) = Cf(r) \tag{32}$$

where  $f(r) = F(r)/(\gamma r)$ ,  $A = A_d + A_q$ ,  $B = B_d + B_q$  and  $C = C_d + C_q$ .

Eq. (31) presents two critical points,  $r_{c1} = 0$  and  $r_{c2} = (-A/B)^{1/2}$ . If a particle is located at critical point  $r_{c1}$ , it will remain trapped at origin. If a particle is located at  $r_{c2}$ , it will describe a circular motion (provided that A/B < 0) of radius  $r_{c2}$  and angular velocity  $C f(r_{c2})$ . Therefore, this result implies that the electromagnetic field given by Eqs. (1), (2) transfers angular momentum to particles that describe a circular motion whose angular velocity is determined by the adequate selection of dipolar and quadrupolar forces.

If parameter C= 0 then  $F_T^{\theta}(r)$  is zero, so in this case, the force acting on the particle will be central, conservative, and its resulting angular momentum will be null.

We are interested in analyzing the case where  $C \neq 0$ , which implies that  $d\theta/dt \neq 0$  and, as a result, the particle will acquire angular momentum from the electromagnetic field. In this sense, to find the differential equation that describes the path of the Si particle, we use the relation  $dr/d\theta = 1/(d\theta/dt)dr/dt$ ; so, taking into account Eqs. (31)–(32), the trajectory of the particle can be obtained by solving:

$$\frac{dr}{d\theta} = \frac{F_T^r(r)}{F_T^\theta(r)} = A_t r + B_t r^3 \tag{33}$$

being  $A_t = A/C$  and  $B_t = B/C$ .

It is easy to check that Eq. (33) admits four solutions,  $r_1(\theta) = 0$ ;  $r_2(\theta) = r_{c2}$  is related to the initial condition  $r_2(0) = r_{c2}$ ,

$$r_3(\theta) = \frac{r_0}{\left(1 - 2B_t r_0^2 \theta\right)^{\frac{1}{2}}} \tag{34}$$

for the initial condition  $r(0) = r_0$  if  $A_t = 0$ , and:

$$r_4(\theta) = \frac{1}{\left(-\frac{B_t}{A_t} + (\frac{1}{r_0^2} + \frac{B_t}{A_t})exp(-2A_t\theta)\right)^{\frac{1}{2}}}$$
(35)

for the initial condition  $r(0) = r_0$  and  $A_t \neq 0$ .

Solution  $r_1$  implies that particles located at origin remain trapped and solution  $r_2$ , as we have mentioned, implies that the particle describes a circular trajectory. On the other hand, solution  $r_3$ , represents a quasi Lituus spiral,  $r_A$  is a logarithmic spiral if  $B_t = 0$  and a quasi logarithmic spiral if  $B_t \neq 0$ . In this sense, there are different possibilities for spiral trajectories as a function of dipolar and quadrupolar coefficients:

- 1. If  $A_t = 0$  and  $B_t < 0$ , Eq. (34) describes an attractive Lituus spiral towards the origin.
- 2. If  $A_t = 0$  and  $B_t > 0$ , Eq. (34) describes a repulsive Lituus spiral, with an asymptote at  $\theta_m = 1/(2 B_t^2 r_0^2)$ .
- 3. If  $A_t < 0$ , A < 0 and C > 0, Eq. (35) describes an attractive logarithmic spiral towards the origin.
- 4. If  $A_t > 0$ , and B < 0 Eq. (35) describes a repulsive spiral that degenerates into a circular trajectory of radius equal to the previously described  $r_{c2} = (-A/B)^{1/2}$
- 5. If  $A_t > 0$ , and B > 0 Eq. (35) describes a repulsive spiral, with an asymptote at  $\theta_l = -1/(2A_t)log(r_0^2/(r_0^2 + A/B))$ .

In cases 1 and 3, particles are trapped at origin, but the convergence dynamic to this point is different, being a function of the balance of dipole and quadrupole coefficients. In case 4, particles describe a final circular movement with angular velocity  $Cf(r_c)$ ; this radius and angular velocity can be modified by the adequate selection of wavelength, which also balances the quadrupolar and dipolar forces. Finally, in cases 2 and 5, particles are repelled towards the outer area of the focal plane.

#### 3. Numerical examples

In this section, we are going to numerically analyze the dynamics of Si nanoparticles immersed in water when two counter-propagating Gaussian beams, with a beam waist radius  $w_0 = 2 \mu m$ , are propagating at different wavelengths and with total incident power of 100 mW. We solve the Langevin equation analyzing orbital stability under Brownian

Fig. 1 shows the quadrupolar  $\mathbf{F}_a$  and dipolar radial forces  $\mathbf{F}_d$  for a Si particle located at  $r = w_0/2$ . As can be observed, quadrupolar forces open a narrow window (this window is narrower and less effective for shorter wavelengths), and for infrared wavelengths, there are attractive interactions that correspond to dipolar repulsive forces resulting in a quadrupolar trap, this being independent from the azimuthal coordinate of particles, as can be deduced from Eqs. (12)-(13). This result was obtained in Ref. [30] for the visible region only using a unique linearly polarized Gaussian beam. We are interested in the analysis of the previously described particle dynamics with strong resonances at infrared region. In this sense, we have fixed the particle radius to 204 nm, which according to Fig. 2(a) shows strong dipolar-quadrupolar magnetic resonance at 1064 nm wavelength, which it is the most common wavelength used in optical traps, as indicated in a recent study of Si nanoparticles forces in the infrared region [34]. Fig. 2(b) shows the coefficients A, B, C for a Si particle of radius 204 nm immersed in water. As can be observed, coefficient A is non null at nearly all the wavelengths of the studied region except for  $\lambda_{A1} = 1046.1$  nm and  $\lambda_{A2}=1097.9$  nm. Moreover, A<0 if  $\lambda\in[\lambda_{A1},\lambda_{A2}]$  and is positive for the rest of the wavelengths. In addition, B>0 if  $\lambda<\lambda_B$  and B<0for  $\lambda > \lambda_B \lambda_B = 1063$  nm being the wavelength for which parameter B is null. Finally, C is positive in the wavelength region  $\lambda > \lambda_C$  where  $\lambda_C = 858.27$  nm and corresponds to the wavelength at which C = 0.

L. Carretero et al. Results in Physics 19 (2020) 103520

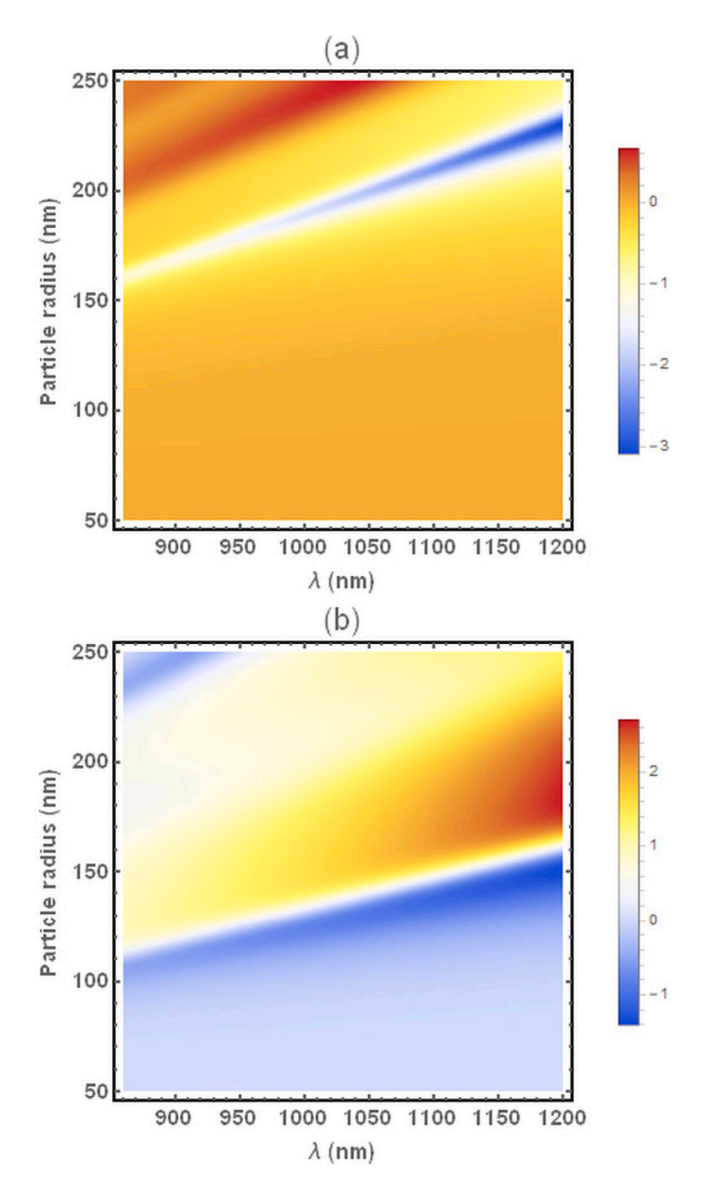


**Fig. 1.** Quadrupolar (a) and dipolar (b) forces for a Si particle located at  $r = w_0/2$ . Scale colors are given in pN. (For interpretation of the references to colour in this figure legend, the reader is referred to the web version of this article.)

Taking into account Eqs. (21)-(29), Fig. 3 shows the different multipolar contributions given to the quadrupolar and dipolar coefficients A, B and C depicted in Fig. 2(b). As can be observed in Fig. 3(a), the contribution of the electric dipolar force to  $A_d$  is negligible and the main contributions are due to the dipolar magnetic force  $A_m$ , and for high wavelength values, the magnetic-electric dipolar interference force  $A_{pm}$ . On the other hand, the major contributions to  $A_q$  arise from quadrupolar electric forces  $A_O$  and magnetic quadrupole-dipole interference force  $A_{Mm}$ , the influence of electric quadrupole-dipole interference  $A_{Op}$  and magnetic quadrupole  $A_M$  being negligible. Thus, taking into account these considerations,  $A \approx A_m + A_{pm} + A_O + A_{Mm}$ . In the same way,  $B_d$  is equal to  $B_p$  being  $B_m = B_{pm} = 0$ . As for the quadrupolar coefficient  $B_q$ , it can be observed in Fig. 3(b) that the main contributions are given by the magnetic quadrupole force  $B_M$ , and electric quadrupolar force  $\mathcal{B}_Q$  whereas the values of  $\mathcal{B}_{Qp}$  are less significant, and hence  $B \approx B_p + B_M + B_Q$ . Finally, it can be deduced from Fig. 3(c) that  $C_d = C_{pm}$  and there is no contribution of dielectric forces because  $C_p \approx 0$ . The quadrupolar coefficient  $C_q$  is practically equal to  $C_{Mm}$  with little corrections due to  $C_{Op}$ . The contribution of

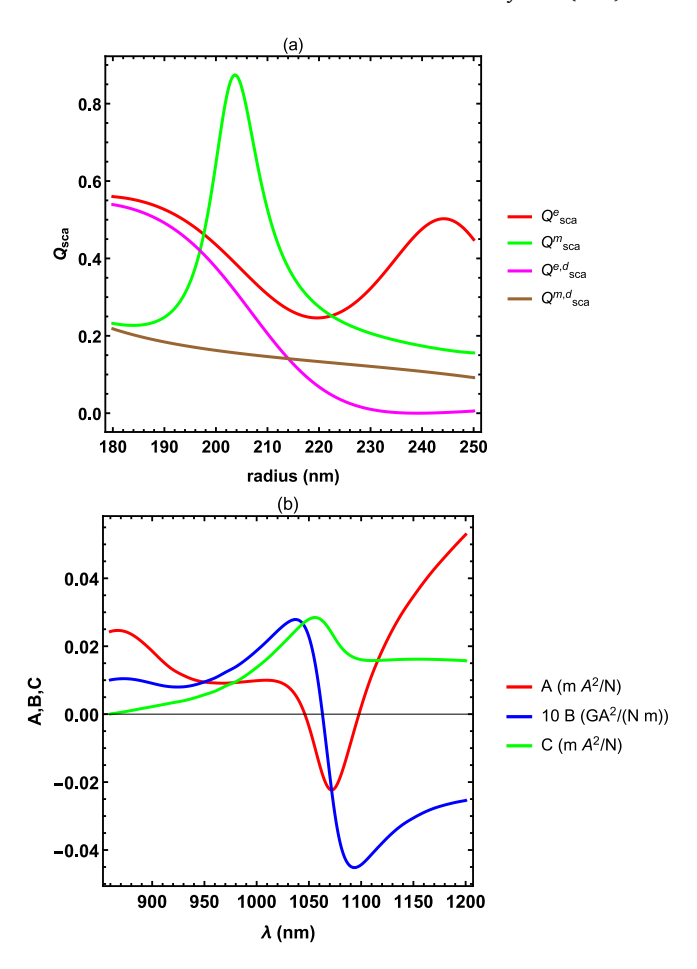


**Fig. 2.** (a) Total electric  $(Q^e_{sca})$  and magnetic  $(Q^m_{sca})$  scattering efficiency including dipolar and quadrupolar terms and dipolar electric  $(Q^{ecd}_{sca})$  and magnetic  $(Q^{md}_{sca})$  scattering efficiency. (b) Coefficients A, B, C for a Si particle of 204 nm radius immersed in water.

magnetic quadrupolar forces  $(C_M)$  is negligible, so  $C=C_{pm}+C_{Mm}+C_{Qp}$  and thus the parameter C mainly depends on the interference forces of dipole–dipole and dipole–quadrupole; i.e. the angular momentum transfer from the electromagnetic field to the particle will be given by interference forces  $\mathbf{F}_{pm}$ ,  $\mathbf{F}_{Op}$  and  $\mathbf{F}_{Mm}$ .

Assuming that the initial position of particle is at  $r = w_0/2$ , Fig. 4, shows the radial and azimuthal forces for a Si nanoparticle of radius 204 nm. As can be seen in Fig. 4(a), the dipolar force is always positive and the quadrupolar force is negative, the resulting total force being repulsive in all the analyzed wavelength spectrum except for the spectral interval that coincides with  $\lambda \in [\lambda_{A1}, \lambda_{A2}]$  (with an error below 0.5 nm, in this zone the parameter A < 0 is accomplished, see Fig. 2(b)), where quadrupolar force dominates and an optical trap is obtained. This result is similar to the one obtained by Xu et al. [30], although they studied the particle dynamic of Si by sorting them by means of Kerker forces using only one linearly polarized Gaussian beam. In our case, Kerker forces ( $\mathbf{F}_{pm}$ ) are included in the dipolar forces, and are not null, unlike with a single circularly polarized Gaussian beam. In one beam configuration, as pointed out in Ref. [30], radiation pressure dominates in the axial direction and thus the particles are not confined at the focus plane. In our configuration, particles are trapped at plane z = 0, where we are going to analyze their dynamic behavior.

Fig. 4(b), shows the azimuthal forces, and as can be observed, the total force is positive for wavelengths  $\lambda \ge \lambda_C$  nm.

When dipolar and quadrupolar azimuthal forces have the same value but with opposite sign  $\lambda=\lambda_C$ , there is no angular momentum transfer from the electromagnetic field to particles and they will

L. Carretero et al. Results in Physics 19 (2020) 103520

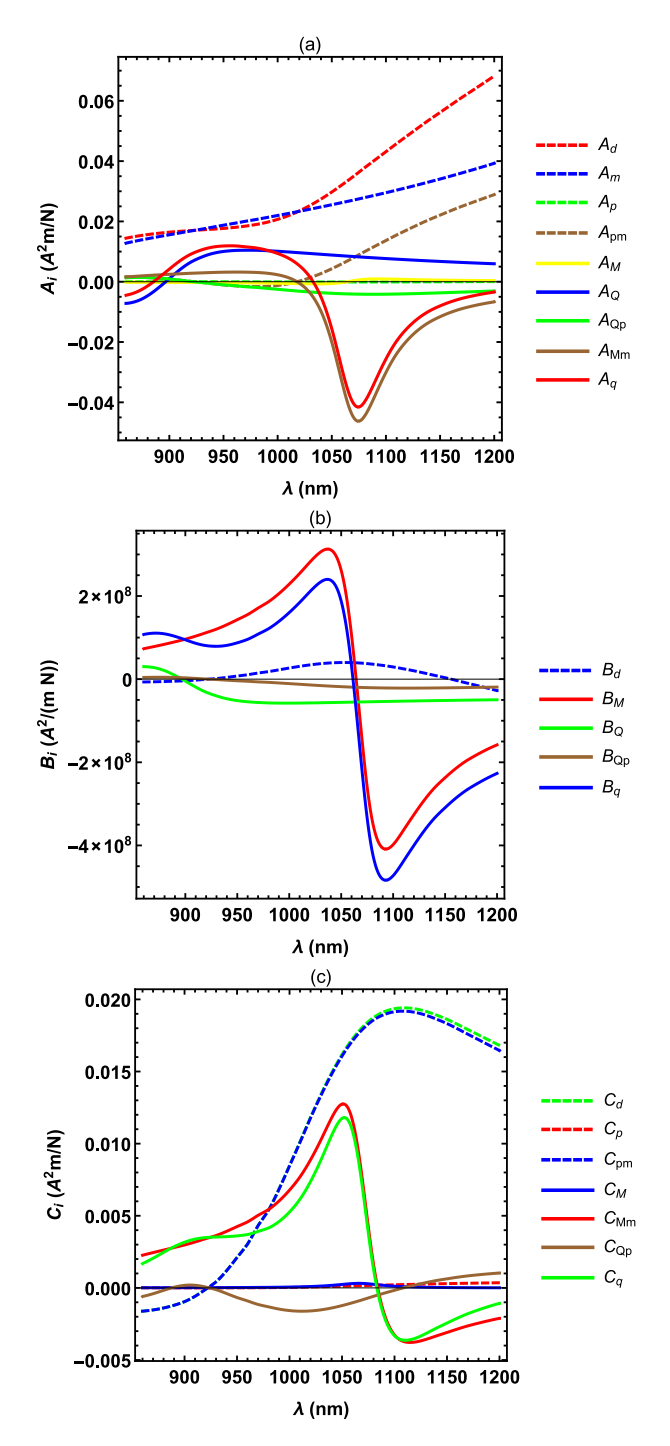


**Fig. 3.** (a) Contributions to  $A_d$  (dashed) and  $A_q$  (continuous), (b) contributions to  $B_d$  (dashed) and  $B_q$  (continuous) and (c) contributions to  $C_d$  (dashed) and  $C_q$  (continuous).

describe a rectilinear motion at focus plane. The transfer of angular momentum will be maximum at  $\lambda_{M2}=1057$  nm which corresponds to the wavelength where C and  $F_{\theta}$  reach the maximum value, the contribution of quadrupolar forces to momentum being nearly 40% of the total. At wavelength  $\lambda_{M1}=922.1$  nm, the angular momentum that a particle acquires is only produced by quadrupolar forces, and for wavelength  $\lambda_{M3}=1083$  nm, the angular momentum transfer to particle is only generated by dipolar forces. Moreover, if the angular momentum of particles is only given by the quadrupolar forces at wavelength  $\lambda_{M1}$ , then  $C_d=0$ , and according to the previous discussion that  $C_{pm}=0$ ;

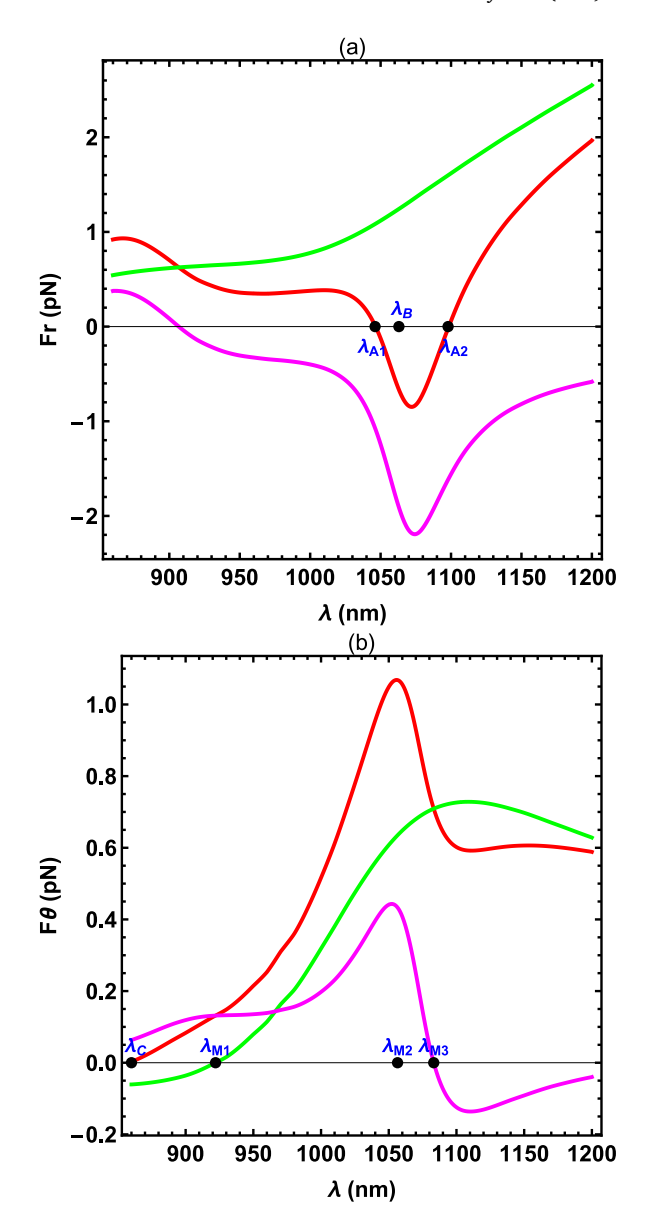


**Fig. 4.** (a) Total radial force (red color), dipolar force (green color) and quadrupolar force (magenta color). (b) Total azimuthal force (red color), dipolar force (green color) and quadrupolar force (magenta color). (For interpretation of the references to colour in this figure legend, the reader is referred to the web version of this article.)

hence, the particle angular momentum is obtained from the interference of quadrupole–dipole forces. On the other hand, when dipolar forces dominate, the main contribution to the angular momentum transfer at wavelength  $\lambda_{M3}$ , is given by the interaction dipole–dipole  $C_{pm}$ , since, in this case, the interference forces of quadrupole–dipole cancel each other as  $C_{Mm} = -C_{Qp}$ .

Fig. 5 shows the trajectories of different particles located at different radial and angular positions at focus plane for wavelengths  $\lambda_C$  (a),  $\lambda_{M1}$  (b),  $\lambda_{M2}$  (c) and  $\lambda_{M3}$  (d). As can be observed, when  $\lambda = \lambda_C$  (Fig. 5(a)), the trajectories are repulsive straight lines, which confirms that there is no transfer of angular momentum from the electromagnetic field to particles. As the wavelength increases, C increases too and particles describe different types of spirals. These trajectories are repulsive for  $\lambda = \lambda_{M1}$ , at which the transfer of angular momentum is only produced by quadrupolar forces, because  $A_i > 0$  and B > 0 (previously described case 5). Furthermore, attractive quasi logarithmic spirals towards the origin with counter-clockwise rotation direction are obtained at  $\lambda =$ 

L. Carretero et al. Results in Physics 19 (2020) 103520

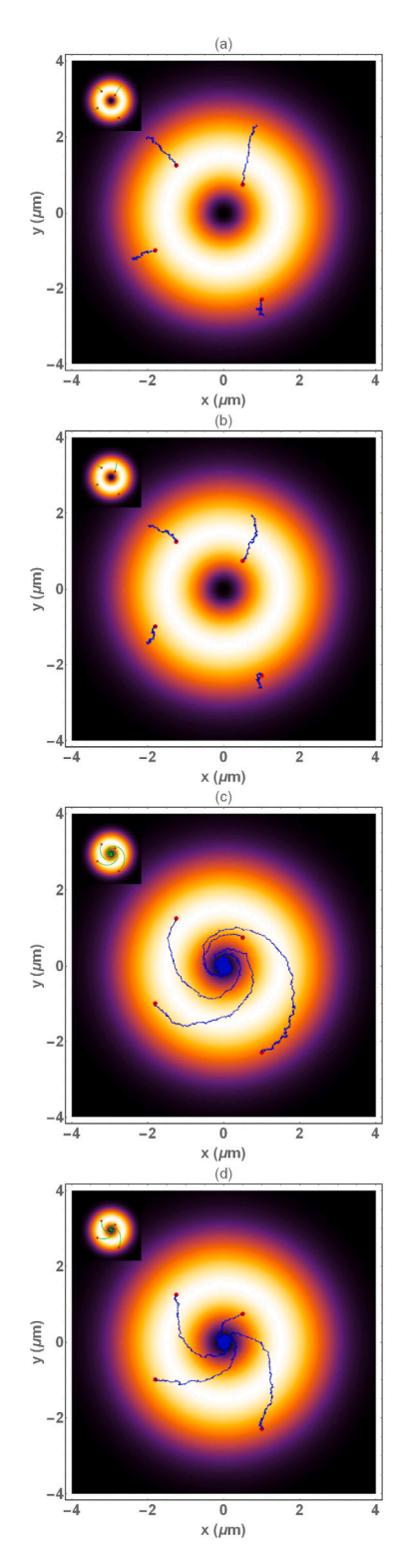


**Fig. 5.** Trajectories described by Si nanoparticles with 203 nm radius for (a)  $\lambda = \lambda_C$ , (b)  $\lambda = \lambda_{M1}$ , (c)  $\lambda = \lambda_{M2}$  and (d)  $\lambda = \lambda_{M3}$ . Red dots indicate the initial position of particle at focus plane. The inset figure shows the deterministic solution of the Langevin equation obtained in Section 2. The simulation time in Figs. 5(a) and (b) is 10 ms, whereas in Figs. 5 (c) and (d) is 100 ms with a time step of 1  $\mu$ s.

 $\lambda_{M2} = \lambda_{M3}$ , which corresponds to case 3 analyzed in Section 2. As can be seen, the deterministic solutions of the Langevin equation (straight lines or spirals) are also observed when the Brownian movement is included. It is interesting to note that trajectories have been represented

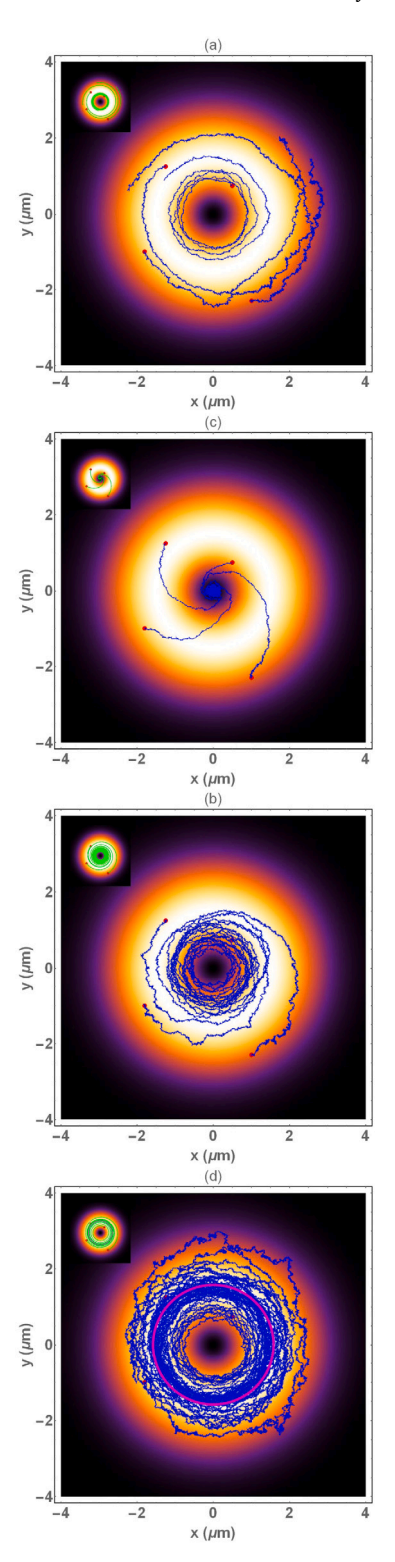


**Fig. 6.** Trajectories described by Si nanoparticles with 203 nm radius for (a)  $\lambda = \lambda_{A1}$ , (b)  $\lambda = \lambda_{A2}$ , (c)  $\lambda = \lambda_B$  and (d)  $\lambda = 1099$  nm. Red dots indicate the initial position of particle at focus plane. The inset figure shows the deterministic solution of the Langevin equation obtained in Section 2. The simulation time in figures is 100 ms with a time step of 1  $\mu$ s, except figure d, for which it has a duration of 1 s.

on the electromagnetic density energy, which shows an optical vortex at origin.

Fig. 6 shows attractive and repulsive Lituus spirals Figs. 6(a) and 6(b) by using illumination wavelengths  $\lambda_{A1}$  and  $\lambda_{A2}$ , respectively. In

both cases, particle radial velocity is much lower than that obtained with the logarithmic spiral shown in Fig. 6(c) corresponding to a wavelength  $\lambda_B$ , because, as can be observed in Fig. 4, the radial force is nearly null in Figs. 6(a) and 6(b). Finally, Fig. 6(d) shows the trajectories that correspond to an illumination with a wavelength of 1099 nm. In this case, according to Figs. 4 and 2 we are under the conditions of case 4, so deterministic orbits converge to a limit cycle that describes a circular movement of radius  $r_{c2} = (-A/B)^{1/2}$  and angular velocity C  $f(r_{c_2})$ . As can be observed, when the Brownian movement is included the circular trajectory (magenta circle) is not stable, but all particles are confined in a region close to this limit cycle, describing spirals around it.

#### 4. Conclusion

The dynamic of Si nanoparticles in a quadrupolar optical trap have been analyzed for different wavelengths in the infrared region. For this purpose, we have obtained the optical forces (characterized by a set of parameters) generated by two counterpropagating circularly polarized Gaussian beams. By solving the deterministic over-damped Langevin equation, we have analytically demonstrated that particles inside the trap describe different types of spirals (attractive or repulsive to the center of the focus), straight lines or circles that are observable with Brownian motion. Through the analysis of the parameters and trajectories, we have demonstrated that the angular momentum transfer is mainly due to the interference forces of dipole–dipole and quadrupole–dipole. In the counter-propagation configuration used particles are trapped at focus plane, so this system could be used in devices to repel or trap particles as a function of wavelength; i.e. it can act as a filter or a purification procedure.

#### CRediT authorship contribution statement

Luis Carretero: Conceptualization, Writing - original draft, Supervision. Pablo Acebal: Investigation, Methodology. Salvador Blaya: Writing - review & editing, Software. Manuel Pérez-Molina: Formal analysis, Writing - review & editing.

#### Declaration of competing interest

The authors declare that they have no known competing financial interests or personal relationships that could have appeared to influence the work reported in this paper.

#### References

- [1] Shilkin DA, Lyubin EV, Shcherbakov MR, Lapine M, Fedyanin AA. Directional optical sorting of silicon nanoparticles. ACS Photon 2017;4(9):2312–9. http: //dx.doi.org/10.1021/acsphotonics.7b00574.
- [2] Vece MD. Using nanoparticles as a bottom-up approach to increase solar cell efficiency. KONA Powder Particle J 2019;36:72–87. http://dx.doi.org/10.14356/ kona.2019005.
- [3] Allen L, Beijersbergen MW, Spreeuw RJC, Woerdman JP. Orbital angular momentum of light and the transformation of laguerre-gaussian laser modes. Phys. Rev. A 1992;45:8185–9. http://dx.doi.org/10.1103/PhysRevA.45.8185.
- [4] H.D.R. Borhen CF. Absorption and scattering of light by small particles. John Wilev & Sons: 1983.
- [5] Nieto-Vesperinas M, Sáenz JJ, Gómez-Medina R, Chantada L. Optical forces on small magnetodielectric particles. Opt Express 2010;18(11):11428–43. http:// dx.doi.org/10.1364/OE.18.011428, URL http://www.opticsexpress.org/abstract. cfm?URI=oe-18-11-11428.
- [6] Bekshaev AY. Subwavelength particles in an inhomogeneous light field: optical forces associated with the spin and orbital energy flows. J Optics 2013;15(4):044004. http://dx.doi.org/10.1088/2040-8978/15/4/044004.
- [7] Bliokh KY, Nori F. Transverse and longitudinal angular momenta of light. Phys Rep 2015;592:1–38. http://dx.doi.org/10.1016/j.physrep.2015.06.003, URL http://www.sciencedirect.com/science/article/pii/S0370157315003336.
- [8] Tamura M, Omatsu T, Tokonami S, Iida T. Interparticle-interaction-mediated anomalous acceleration of nanoparticles under light-field with coupled orbital and spin angular momentum. Nano Lett 2019;19(8):4873–8, pMID: 31272154. http://dx.doi.org/10.1021/acs.nanolett.9b00332.

[9] Li M, Yan S, Yao B, Liang Y, Zhang P. Spinning and orbiting motion of particles in vortex beams with circular or radial polarizations. Opt Express 2016;24(18):20604–12. http://dx.doi.org/10.1364/OE.24.020604, URL http:// www.opticsexpress.org/abstract.cfm?URI=oe-24-18-20604.

- [10] Yu H, She W. Radiation torques exerted on a sphere by focused laguerre-gaussian beams. Phys Rev A 2015;92:023844. http://dx.doi.org/10.1103/PhysRevA.92. 023844
- [11] Cai W, Reinhardt O, Kaminer I, de Abajo FJG. Efficient orbital angular momentum transfer between plasmons and free electrons. Phys Rev B 2018;98:045424. http://dx.doi.org/10.1103/PhysRevB.98.045424.
- [12] Angelsky OV, Bekshaev AY, Maksimyak PP, Maksimyak AP, Mokhun II, Hanson SG, Zenkova CY, Tyurin AV. Circular motion of particles suspended in a gaussian beam with circular polarization validates the spin part of the internal energy flow. Opt Express 2012;20(10):11351-6. http://dx.doi.org/10.1364/OE.20.011351, URL http://www.opticsexpress.org/abstract.cfm?URI=oe-20-10-11351
- [13] Angelsky OV, Bekshaev AY, Maksimyak PP, Maksimyak AP, Hanson SG, Zenkova CY. Orbital rotation without orbital angular momentum: mechanical action of the spin part of the internal energy flow in light beams. Opt Express 2012;20(4):3563–71. http://dx.doi.org/10.1364/OE.20.003563, URL http://www.opticsexpress.org/abstract.cfm?URI=oe-20-4-3563.
- [14] Svak V, Brzobohatý O, Šiler, Jàkl P, Kaňka J, Zemànek P, Simpson SH. Transverse spin forces and non-equilibrium particle dynamics in a circularly polarized vacuum optical trap. Nature Commun 2018;9(4):5453. http://dx.doi.org/10. 1364/OE.20.003563, URL http://www.opticsexpress.org/abstract.cfm?URI=oe-20-4-3563.
- [15] Bekshaev A, Bliokh KY, Soskin M. Internal flows and energy circulation in light beams. J Optics 2011;13(5):053001. http://dx.doi.org/10.1088/2040-8978/13/ 5/053001.
- [16] Zhao Y, Edgar JS, Jeffries GDM, McGloin D, Chiu DT. Spin-to-orbital angular momentum conversion in a strongly focused optical beam. Phys Rev Lett 2007;99:073901. http://dx.doi.org/10.1103/PhysRevLett.99.073901.
- [17] Zemánek P, Volpe G, Jonáš A, Brzobohatý O. Perspective on light-induced transport of particles: from optical forces to phoretic motion. Adv Opt Photon 2019;11(3):577–678. http://dx.doi.org/10.1364/AOP.11.000577, URL http://aop.osa.org/abstract.cfm?URI=aop-11-3-577.
- [18] Milne G, Dholakia K, McGloin D, Volke-Sepulveda K, Zemánek P. Transverse particle dynamics in a bessel beam. Opt Express 2007;15(21):13972–87. http:// dx.doi.org/10.1364/OE.15.013972, URL http://www.opticsexpress.org/abstract. cfm?URl=oe-15-21-13972.
- [19] Hay RF, Gibson GM, Simpson SH, Padgett MJ, Phillips DB. Lissajous-like trajectories in optical tweezers. Opt Express 2015;23(25):31716–27. http:// dx.doi.org/10.1364/OE.23.031716, URL http://www.opticsexpress.org/abstract. cfm?URl=oe-23-25-31716.
- [20] Mazilu M, Arita Y, Vettenburg T, Auñón JM, Wright EM, Dholakia K. Orbitalangular-momentum transfer to optically levitated microparticles in vacuum. Phys Rev A 2016;94:053821. http://dx.doi.org/10.1103/PhysRevA.94.053821.
- [21] Ng J, Lin Z, Chan CT. Theory of optical trapping by an optical vortex beam. Phys Rev Lett 2010;104:103601. http://dx.doi.org/10.1103/PhysRevLett.104.103601.
- [22] Wang N, Chen J, Liu S, Lin Z. Dynamical and phase-diagram study on stable optical pulling force in bessel beams. Phys Rev A 2013;87:063812. http://dx. doi.org/10.1103/PhysRevA.87.063812.
- [23] Ashkin A. Acceleration and trapping of particles by radiation pressure. Phys Rev Lett 1970;24:156–9. http://dx.doi.org/10.1103/PhysRevLett.24.156.
- [24] Donato MG, Brzobohatý O, Simpson SH, Irrera A, Leonardi AA, Lo Faro MJ, Svak V, Maragò OM, Zemánek P. Optical trapping optical binding and rotational dynamics of silicon nanowires in counter-propagating beams. Nano Lett 2019;19(1):342–52. http://dx.doi.org/10.1021/acs.nanolett.8b03978.
- [25] Wang X, Rui G, Gong L, Gu B, Cui Y. Manipulation of resonant metallic nanoparticle using 4pi focusing system. Opt Express 2016;24(21):24143–52. http://dx.doi.org/10.1364/OE.24.024143, URL http://www.opticsexpress.org/abstract.cfm?URI=oe-24-21-24143.
- [26] Vázquez-Lozano JE, Martínez A, Rodríguez-Fortuño FJ. Near-field directionality beyond the dipole approximation: Electric quadrupole and higher-order multipole angular spectra. Phys Rev Appl 2019;12:024065. http://dx.doi.org/10.1103/ PhysRevApplied.12.024065.
- [27] Chen J, Ng J, Lin Z, Chan C. Optical pulling force. Nature Photon 2011;5:531-4.
- [28] Babicheva VE, Evlyukhin AB. Analytical model of resonant electromagnetic dipole-quadrupole coupling in nanoparticle arrays. Phys Rev B 2019;99:195444. http://dx.doi.org/10.1103/PhysRevB.99.195444.
- [29] Grinter R, Jones GA. Interpreting angular momentum transfer between electromagnetic multipoles using vector spherical harmonics. Opt Lett 2018;43(3):367–70. http://dx.doi.org/10.1364/OL.43.000367, URL http://ol.osa.org/abstract.cfm?URI=ol-43-3-367.
- [30] Xu X, Nieto-Vesperinas M, Qiu C-W, Liu X, Gao D, Zhang Y, Li B. Kerker-type intensity-gradient force of light. Laser Photonics Rev 2020;14(4):1900265. http://dx.doi.org/10.1002/lpor.201900265. arXiv: https://onlinelibrary.wiley.com/doi/pdf/10.1002/lpor.201900265. URL https://onlinelibrary.wiley.com/doi/abs/10.1002/lpor.201900265.

- [31] Hauss HA. Solid state physical electronics. In: Nick Holonyak J, editor. Waves and fields in optoelectronics. Prentice-Hall; 1984.
- [32] Sandric N. Stability of the overdamped langevin equation in double-well potential. J Math Anal Appl 2018;467(1):734–50. http://dx.doi.org/10. 1016/j.jmaa.2018.07.043, URL http://www.sciencedirect.com/science/article/pii/S0022247X18306255.
- [33] Carretero L, Acebal P, Garcia C, Blaya S. Periodic trajectories obtained with an active tractor beam using azimuthal polarization: Design of particle exchanger. IEEE Photonics J 2015;7(1):1–12.
- [34] Länk NO, Johansson P, Käll M. Directional scattering and multipolar contributions to optical forces on silicon nanoparticles in focused laser beams. Opt Express 2018;26(22):29074–85. http://dx.doi.org/10.1364/OE.26.029074, URL http://www.opticsexpress.org/abstract.cfm?URI=oe-26-22-29074.